

Randall-Sundrum Reality at the LHC

Vernon Barger^a and Muneyuki Ishida^b

^a*Department of Physics, University of Wisconsin, Madison, WI 53706, USA*

^b*Department of Physics, Meisei University, Hino, Tokyo 191-8506, Japan*

Abstract

The radion is expected to be the first signal of the Randall-Sundrum (RS) model. We explore the possibility of finding it in the ongoing Higgs searches at the LHC. The little RS model (LRS), which has a fundamental scale at $\sim 10^3$ TeV, is excluded over wide ranges of the radion mass from the latest WW and $\gamma\gamma$ data by ATLAS and CMS.

Key words: radion, RS model, LHC

PACS: 04.50.-h, 11.10.Kk

1 Introduction

The standard model (SM) successfully explains almost all present experimental data; however, it is an unsatisfactory model to be the ultimate theory of particle physics. One of its defects is a large hierarchy between the two fundamental scales, the Planck scale $M_{Pl} \simeq 2 \times 10^{18}$ GeV and the weak scale ~ 100 GeV, which requires an unnatural fine-tuning of model-parameters when the model is applied to weak-scale phenomenology. The Randall-Sundrum model[1] was originally proposed to solve this hierarchy problem. RS introduced the five-dimensional anti-de Sitter spacetime,

$$ds^2 = e^{-2ky} \eta_{\mu\nu} dx^\mu dx^\nu - dy^2, \quad (1)$$

with a S^1/Z_2 compactified 5-th dimension, denoted as $y \in [0, L]$; there are two three-branes at $y = 0$ and $y = L$, called UV and IR branes, respectively. All the SM fields are confined to the IR brane in the original setup of Randall-Sundrum model, denoted as the RS1 model, and the 5-dimensional fundamental scale M_5 at UV brane is scaled down to $M_5 e^{-kL}$ at the IR brane by the warp factor e^{-kL} appearing in the metric of Eq. (1). By taking $kL \simeq 35$,

the fundamental scale $M_5 = M_{Pl}$ is scaled down to the TeV scale. In order to suppress unwanted higher dimensional operators, which are not sufficiently suppressed by the TeV-scale cutoff on the IR brane in the RS1 model, SM gauge fields[2,3,4,5] and fermions[6,7] are considered to propagate in the bulk space. In this new setup[2,3,4,5,6,7,8,9,10,11,12,13,14,15,16], denoted as the RS model, RS can address both the hierarchy problem and fermion mass hierarchies. From the electroweak precision measurements and various flavor physics, the new Kaluza-Klein (KK) modes of the bulk SM fields are constrained to be heavier than a few TeV[2,3,4,5,6,7,8,9,10,11,12,13,14,15,16,17,18,19,20,21,22].

The radion ϕ was introduced as a quantum fluctuation of the modulus L of the 5-th dimension. It is necessary to stabilize L to the above value. Goldberger and Wise showed that a bulk scalar field propagating in the background geometry, Eq. (1), can generate a potential that can stabilize L . [23] In order to reproduce the value $kL \simeq 35$, the radion should have a lighter mass than those of any other Kaluza-Klein modes of all bulk fields[24]. Thus, the detection of the radion may well be expected as the first signal to indicate that the RS model is truly realized in nature.

From a purely phenomenological perspective, the fundamental scale M_5 is scaled down far below the 4-dimensional M_{Pl} , by reducing the volume kL of 5-th dimension. This is known as little Randall-Sundrum (LRS) model[25]. The hierarchy problem is yet unsolved in this model. The neutral kaon mixing parameter ϵ_K gives a strong constraint[26] on M_5 , namely $M_5 >$ several thousand TeV, in the LRS model, and this corresponds to $kL \geq 7$. The present precision measurements of SM flavors are consistent with $kL = 7$. The diphoton signal at the LHC is predicted to be largely enhanced[27] in comparison with the RS model with $kL = 35$.

In this Letter we evaluate the production and decays of the radion. Similar analyses were done in ref.[5,27,28,29,30,31,32]. We refine the calculations appropriate to the LHC experiments at 7 TeV (LHC7), and consider the possibility of finding ϕ in the ongoing LHC Higgs searches. We demonstrate that ϕ could be found in the SM Higgs search in the $\gamma\gamma$ and W^*W^* channels at LHC7, and consider the possibility of RS and LRS models being thereby tested. We find that the LRS model with $kL = 7$ is excluded by the latest ATLAS and CMS data over wide ranges of the radion mass.

2 Coupling to the SM particles

We define the fluctuation F of the metric and the canonically normalized radion field ϕ as

$$\begin{aligned}
ds^2 &= e^{-2(ky+F)} \eta_{\mu\nu} dx^\mu dx^\nu - (1+2F)^2 dy^2, \\
F &= \frac{\phi(x)}{\Lambda_\phi} e^{2k(y-L)},
\end{aligned} \tag{2}$$

where Λ_ϕ is the VEV of the radion field $\phi(x)$.

The couplings of the radion to the SM particles in the original RS model are composed of two parts,

$$L = L_{trace} + L_{bulk}, \tag{3}$$

where L_{trace} is determined from general covariance[23,28,29] to be

$$\begin{aligned}
L_{trace} &= \frac{\phi}{\Lambda_\phi} T_\mu^\mu(SM). \\
T_\mu^\mu(SM) &= T_\mu^\mu(SM)^{\text{tree}} + T_\mu^\mu(SM)^{\text{anom}} \\
T_\mu^\mu(SM)^{\text{tree}} &= \sum_f m_f \bar{f} f - 2m_W^2 W_\mu^+ W^{-\mu} - m_Z^2 Z_\mu Z^\mu + 2m_h^2 h^2 - \partial_\mu h \partial^\mu h \\
T_\mu^\mu(SM)^{\text{anom}} &= -\frac{\alpha_s}{8\pi} b_{QCD} \sum_a F_{\mu\nu}^a F^{a\mu\nu} - \frac{\alpha}{8\pi} b_{EM} F_{\mu\nu} F^{\mu\nu}.
\end{aligned} \tag{4}$$

Here $T_\mu^\mu(SM)$, the trace of the SM energy-momentum tensor, which is defined by $\sqrt{-g}T_{\mu\nu}(SM) = 2\frac{\delta(\sqrt{-g}L_{SM})}{\delta g^{\mu\nu}}$, is represented as a sum of the tree-level term $T_\mu^\mu(SM)^{\text{tree}}$ and the trace anomaly term $T_\mu^\mu(SM)^{\text{anom}}$ for gluons and photons. $F_{\mu\nu}^a(F_{\mu\nu})$ are their field strengths. The b values are $b_{QCD} = 11 - (2/3)6 + F_t$, including the top loop, and $b_{EM} = 19/6 - 41/6 + (8/3)F_t - F_W$, including the top and W loops.¹

The $T_\mu^\mu(SM)^{\text{tree}}$ is proportional to particle masses. The new RS model with the SM fields propagating in the bulk has an additional radion interaction, L_{bulk} , which is inversely proportional to the volume of the 5-th dimension[4,5]. There is a correction to the interactions of fermions, massless gluons and photons that have couplings to a radion in the tree level.

These interactions are very similar form to the interactions of SM Higgs except for an overall proportional constant,² the inverse of the radion interaction scale Λ_ϕ , which is the VEV of ϕ . It is given by

¹ $F_t = \tau_t(1 + (1 - \tau_t)f(\tau_t))$ and $F_W = 2 + 3\tau_W + 3\tau_W(2 - \tau_W)f(\tau_W)$. $f(\tau) = [\text{Arcsin}(\frac{1}{\sqrt{\tau}})]^2$ for $\tau \geq 1$ and $-\frac{1}{4}[\ln\frac{\eta_+}{\eta_-} - i\pi]^2$ for $\tau < 1$ with $\eta_\pm = 1 \pm \sqrt{1 - \tau}$. Here $\tau_i \equiv \left(\frac{2m_i}{m_\phi}\right)^2$ for $i = t, W$.

² An overall sign of the radion couplings is opposite to the Higgs couplings in the most frequently used definition of $\phi(x)$, Eq. (2).

$$\Lambda_\phi = e^{-kL} \sqrt{\frac{6M_5^3}{k}}. \quad (5)$$

We adopt the radion effective interaction Lagrangian given in Ref.[5] The radion couplings to gluons and photons are

$$L_A = -\frac{\phi}{4\Lambda_\phi} \left[\left(\frac{1}{kL} + \frac{\alpha_s}{2\pi} b_{QCD} \right) \sum_a F_{\mu\nu}^a F^{a\ \mu\nu} + \left(\frac{1}{kL} + \frac{\alpha}{2\pi} b_{EM} \right) F_{\mu\nu} F^{\mu\nu} \right] \quad (6)$$

We note that L_A has both contributions from L_{bulk} proportional to $(kL)^{-1}$ and L_{trace} from the trace anomaly term, while only the latter term contributes for the SM Higgs case.

The radion couplings to W, Z bosons are

$$L_V = -\frac{2\phi}{\Lambda_\phi} \left[\left(\mu_W^2 W_\mu^+ W^{-\ \mu} + \frac{1}{4kL} W_{\mu\nu}^+ W^{-\ \mu\nu} \right) + \left(\frac{\mu_Z^2}{2} Z_\mu Z^\mu + \frac{1}{8kL} Z_{\mu\nu} Z^{\mu\nu} \right) \right] \quad (7)$$

where $V_{\mu\nu} = \partial_\mu V_\nu - \partial_\nu V_\mu$ for $V_\mu = W_\mu^\pm, Z_\mu$ and μ_i^2 ($i = W, Z$), which include the contributions from the bulk wave functions of W, Z , are represented by using $W(Z)$ mass $m_{W,Z}$ as $\mu_i^2 = m_i^2 [1 - \frac{kL}{2} (\frac{m_i}{k})^2]$ ³ where $\tilde{k} = k e^{-kL}$ sets a mass scale of KK-excitations.

The radion couplings to the fermions are proportional to their masses.

$$L_f = -\frac{\phi}{\Lambda_\phi} m_f [I(c_L) + I(c_R)] (\bar{f}_L f_R + \bar{f}_R f_L). \quad (8)$$

The coupling is proportional to the other factor $I(c_L) + I(c_R)$ which is dependent upon the bulk profile parameters c_L and c_R . The $I(c_L) + I(c_R)$ are given as $1 \sim 1.19$ and 1 for $b\bar{b}$ and $t\bar{t}, \tau\tau$ channels, respectively, in ref.[5], while the value for $c\bar{c}$ is model-dependent. We simply take $I(c_L) + I(c_R) = 1$ for all the relevant channels of $b\bar{b}, t\bar{t}, \tau\tau, c\bar{c}$.⁴

The coupling of the radion to the IR brane-localized Higgs scalar h is given by

³ The physical masses of W, Z bosons are identified with μ_i , not m_i ($i = W, Z$); however, we neglect small difference between μ_i and m_i , and the m_i 's are fixed with the physical masses.

⁴ $c\bar{c}$ has only a tiny BF . For $b\bar{b}$, the $I(c_L) + I(c_R)$ is given as 1.66 in another example[25]. In this case the $BF(\phi \rightarrow b\bar{b})$ becomes about 2.5 times larger than our present result.

$$L_h = \frac{\phi}{\Lambda_\phi} (-\partial_\mu h \partial^\mu h + 2m_h^2 h^2) . \quad (9)$$

The model parameters are kL , Λ_ϕ , m_ϕ and m_h . In the following we consider two values of kL : $kL = 7$ corresponding to the LRS model and $kL = 35$ to the original RS model. The value $\Lambda_\phi = 3$ TeV is used[27]. k is taken safely as $k < M_5$ in the original RS model[1]. Here we simply take $k = M_5$. From Eq. (5) this corresponds to $\tilde{k} = \Lambda_\phi/\sqrt{6}$. The m_h is taken as 130 GeV unless it is specified, while m_ϕ is treated as a free parameter. By using the effective couplings Eqs. (6) - (9) and these values of parameters, we calculate the partial decay widths and thier branching ratios in §4.

3 Radion Production at the LHC

The production cross section of the radion ϕ at hadron colliders is expected to be mainly via gg fusion, similarly to the production of a Higgs boson h^0 . These cross sections are proportional to the respective partial decay widths to gg . The production cross section of h^0 has been calculated in NNLO[36], and by using this result⁵ we can directly estimate the production cross section of ϕ as

$$\sigma(pp \rightarrow \phi X) = \sigma(pp \rightarrow h^0 X) \times \frac{\Gamma(\phi \rightarrow gg)}{\Gamma(h^0 \rightarrow gg)} . \quad (10)$$

By using the $\Gamma(\phi \rightarrow gg)$ partial width given later and $\Gamma(h^0 \rightarrow gg)$ of the SM we can predict $\sigma(pp \rightarrow \phi X)$ in the two cases $kL = 7, 35$. The result is compared with the SM Higgs production in Fig. 1.

The production of ϕ scales with an overall factor $(1/\Lambda_\phi)^2$. In the $\Lambda_\phi = 3$ TeV case, the production of ϕ in the original RS model ($kL = 35$) is almost the same as that of the SM Higgs boson of the same mass, while in the LRS case ($kL=7$) the radion cross section exceeds that of the SM Higgs. This is because ϕ production from gg fusion has an amplitude that includes a term proportional to $1/kL$ at tree level, while there is no such term in h^0 production. Our prediction of $\sigma(\phi)$ in Fig.1 includes the $\pm 25\%$ uncertainty associated with the theoretical uncertainty on $\sigma(h^0)$ [36].

⁵ The QCD radiative corrections to the tree level $gg \rightarrow h^0$ and $gg \rightarrow \phi$ should be equal in the point-like approximation of the $gg \rightarrow h^0/\phi$ interactions, so we use the tree level result for $\Gamma(\phi \rightarrow gg)/\Gamma(h^0 \rightarrow gg)$.

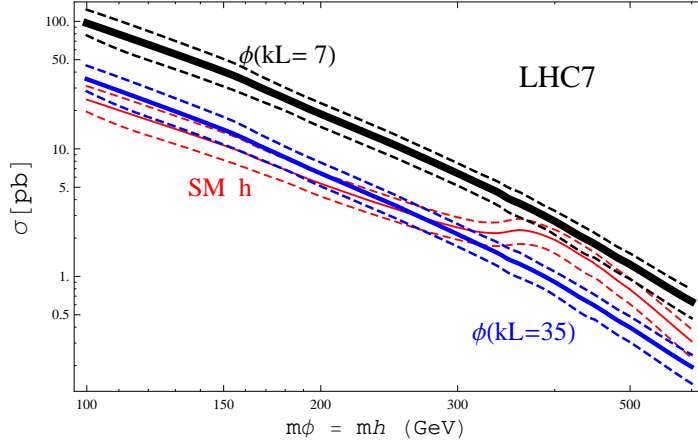


Fig. 1. The production cross sections at LHC7 of the radion ϕ via gg fusion (solid blue $kL = 35$ corresponding to the original RS model and solid thick black $kL = 7$ to LRS model), compared with that of the SM Higgs with the same mass $m_{h^0} = m_\phi$ (solid thin red). The ϕ production cross sections are proportional to inverse-squared of Λ_ϕ , which is taken to be $\Lambda_\phi = 3$ TeV here. The overall theoretical uncertainties[36] are denoted by dotted lines.

4 Radion Decay

For the radion decay channels $\phi \rightarrow AB$, we consider $AB = gg, \gamma\gamma, W^+W^-, ZZ, b\bar{b}, c\bar{c}, \tau^+\tau^-, t\bar{t}$, and h^0h^0 . Their partial widths are given by the formula

$$\Gamma(\phi \rightarrow AB) = \frac{N_c}{8\pi(1 + \delta_{AB})m_\phi^2} p(m_\phi^2; m_A^2, m_B^2) \times |M|^2 \quad (11)$$

where p is the momentum of particle A (or B) in the CM system and $|M|^2$ represents the decay amplitude squared which are given in Table 1.⁶

The results of the decay branching fractions are given for the two cases $kL = 7, 35$ in Fig. 2.

In the $kL = 7$ (LRS model) case, there is a strong enhancement of $BF(\phi \rightarrow \gamma\gamma)$, in comparison with the RS model case with $kL = 35$, as was pointed out in ref.[27]. The $BF(\gamma\gamma)$ reaches almost 10^{-2} in LRS model, while it is $\sim 10^{-4}$ almost independent of m_ϕ in RS model. The $BF(\gamma\gamma)$ is proportional to $(1/kL)^2$

⁶ For the gg decay of ϕ we include the radiative corrections at NNLO by using the K-factor from Higgs production. We use central values of the K-factor given in Fig. 8 of Ref.[37]: For $m_{h^0} = 100 \sim 600$ GeV, $K = 2.0 \sim 2.6$. This value is about 10% larger than the K-factor of Higgs decaying into gg in NNLO given in ref.[44] but within the uncertainty of the choice of the renormalization scale. So we assume the ϕ and h K-factors are equal and adopt the value in ref.[37].

Table 1

Decay amplitudes squared $|M|^2$ of ϕ . $|M|^2$ for ZZ is obtained by replacement $W \rightarrow Z$ from $M_{T,L}^{WW}$. gg includes a K-factor $K(m_\phi)$ [36]. b_{QCD}, b_{EM} are given below Eq. (4) in the text. $b\bar{b}$ includes radiative corrections[39] of running mass $m_b(m_\phi)$ and an overall factor $C(m_\phi)$, but we adopt fixed mass m_b for the kinematical factor $(m_\phi^2/4 - m_b^2)^{3/2}$. Similar expressions are also applied to $t\bar{t}, c\bar{c}$ channels. The off-shell $WW^*(ZZ^*)$ channels in the low-mass ϕ case are treated in the same method as in ref.[38].

decay channel	$ M ^2$
W^+W^-	$2 M_T^{WW} ^2 + M_L^{WW} ^2$
gg	$2 M_T^{gg} ^2 \cdot K(m_\phi)$
$\gamma\gamma$	$2 M_T^{\gamma\gamma} ^2$
$b\bar{b}$	$\frac{8}{\Lambda_\phi^2} C(m_\phi) m_b(m_\phi)^2 (\frac{m_\phi^2}{4} - m_b^2)$
$\tau^+\tau^-$	$\frac{8}{\Lambda_\phi^2} m_\tau^2 (m_\phi^2/4 - m_\tau^2)$
$h^0 h^0$	$ - \frac{1}{\Lambda_\phi} (m_\phi^2 + 2m_{h^0}^2) ^2$
$M_T^{WW} = -\frac{2}{\Lambda_\phi} \left\{ \mu_W^2 - \frac{1}{2kL} \frac{m_\phi^2 - 2m_W^2}{2} \right\}$ $M_L^{WW} = -\left(1 - \frac{m_\phi^2}{2m_W^2}\right) M_T^{WW} - \frac{2}{\Lambda_\phi} \frac{1}{2kL} \frac{m_\phi^2 (m_\phi^2/4 - m_W^2)}{m_W^2}$ $M_T^{gg,\gamma\gamma} = \frac{m_\phi^2}{2\Lambda_\phi kL} \left(1 + \frac{\alpha_s b_{QCD}}{2\pi} kL\right), \quad \frac{m_\phi^2}{2\Lambda_\phi kL} \left(1 + \frac{\alpha b_{EM}}{2\pi} kL\right)$	

in $m_\phi \gtrsim 200$ GeV region in the LRS model.⁷ This huge enhancement is from the bulk field coupling of ϕ proportional to $1/kL$. We do not find sharp dips in $BF(\phi \rightarrow WW, ZZ)$ around $m_\phi \simeq 450$ GeV of Fig. 1 in ref.[27].

The total width of ϕ in Fig.3 is one or two orders of magnitude smaller than that of the SM Higgs with the same mass. This is because the choice of $\Lambda_\phi = 3$ TeV is about one order of magnitude larger than the Higgs VEV $v = 246$ GeV. A ϕ resonance would be observed with the width of the experimental resolution. The $\Gamma(\phi \rightarrow WW)$ partial width is negligibly small compared with $\Gamma(h^0 \rightarrow WW)$, and thus ϕ production via vector boson(WW, ZZ) fusion is unimportant at the LHC, providing another way to distinguish ϕ and h^0 . We note that double Higgs production via ϕ decays would uniquely distinguish ϕ and h .

⁷ It should be noted that in the original RS model setup where the SM fields are confined in the IR brane, $BF(\gamma\gamma)$ steeply decreases with $m_\phi > 200$ GeV similarly to the SM Higgs. This modified behavior comes from L_{bulk} in the new bulk field scenario of SM field.

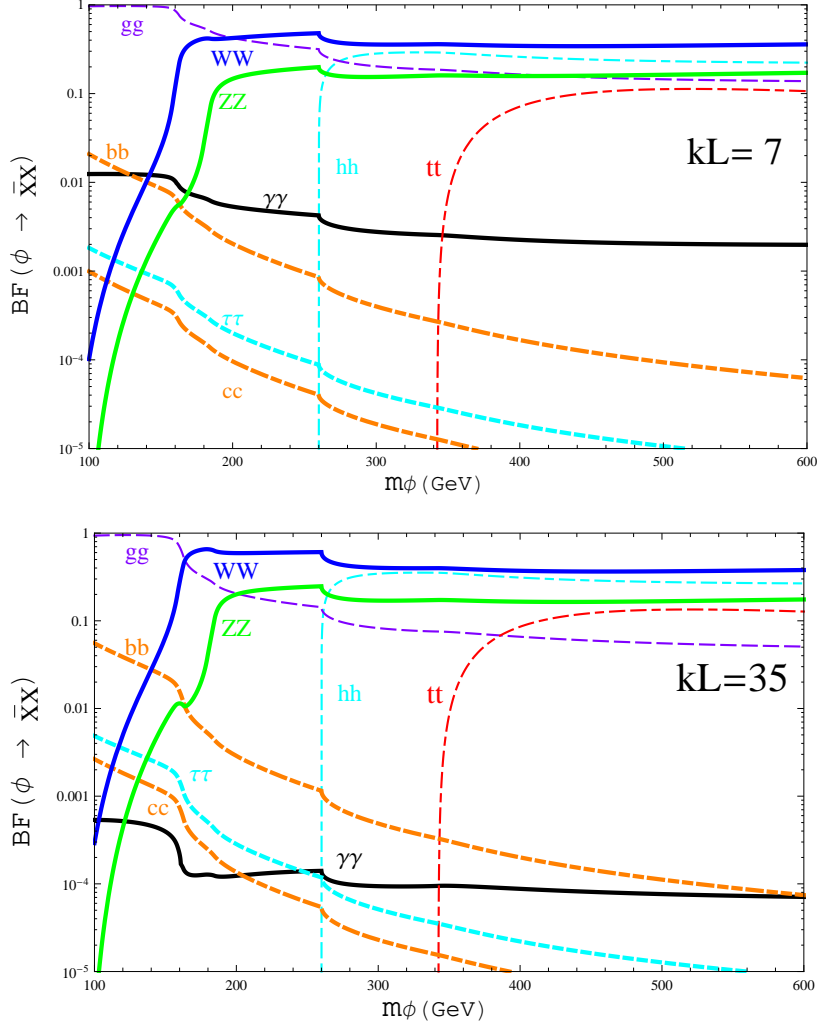


Fig. 2. Decay Branching Fractions of ϕ versus m_ϕ (GeV) for $kL = 7$ (LRS model) and 35(RS model). m_{h^0} is taken to be 150 GeV.

5 Radion Detection compared to SM Higgs

Next we consider the detection of ϕ in the W^+W^- , ZZ and $\gamma\gamma$ decay channels. The ϕ search can be made in conjunction with the Higgs search. The properties of h^0 at the LHC are well known, so we use them as benchmarks of the search for ϕ .

The ϕ detection ratio (DR) to h^0 in the $\bar{X}X$ channel is defined[40] by

$$DR \equiv \frac{\Gamma_{\phi \rightarrow gg} \Gamma_{\phi \rightarrow \bar{X}X} / \Gamma_{\phi}^{\text{tot}}}{\Gamma_{h^0 \rightarrow gg} \Gamma_{h^0 \rightarrow \bar{X}X} / \Gamma_{h^0}^{\text{tot}}}, \quad (12)$$

where $\bar{X}X = W^+W^-$, ZZ , and $\gamma\gamma$. The DR are plotted versus $m_\phi = m_{h^0}$ in

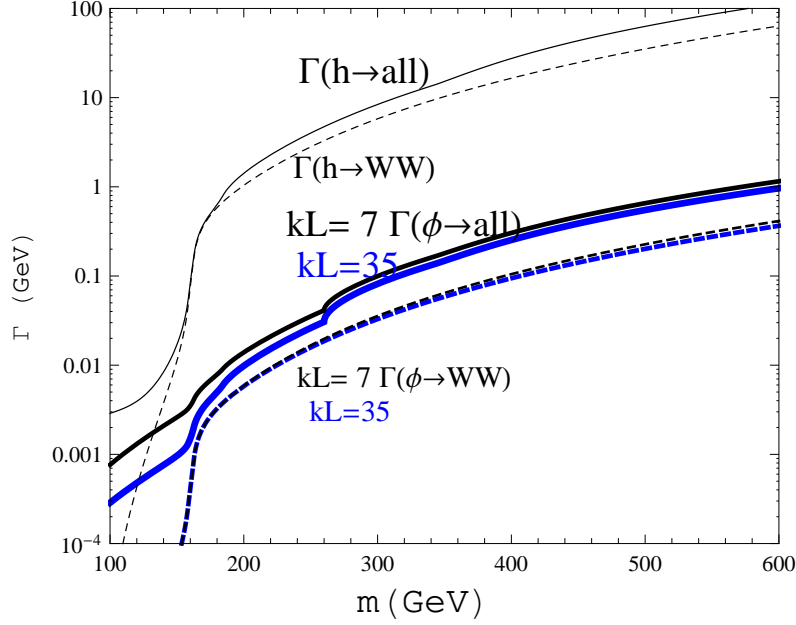


Fig. 3. Total widths (GeV) and W^+W^- partial widths of ϕ compared with the SM higgs h^0 with the same mass $m = m_\phi = m_h$ (GeV). The $\Lambda_\phi = 3$ TeV and $kL = 7, 35$ cases are shown. For $\Gamma(\phi \rightarrow \text{all})$ the m_h is fixed with 130 GeV. The widths of ϕ are proportional to the inverse squared of Λ_ϕ .

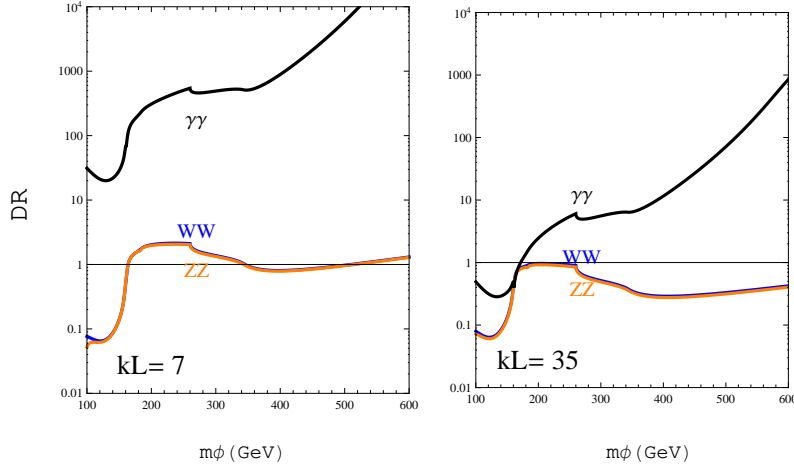


Fig. 4. ϕ Detection Ratio (DR) to the SM higgs h^0 of Eq. (12) for the $\bar{X}X = W^+W^-$ (solid blue), ZZ (dashed orange), and $\gamma\gamma$ (solid black) final states for $kL = 7, 35$ versus m_ϕ (GeV).

Fig. 4 for the two cases $kL = 7$ and 35.

In mass range between the WW threshold and the h^0h^0 threshold (300 GeV in the present illustration) the ϕ to h^0 detection ratio is relatively large in both WW and ZZ channels. The DR is almost 2 in the $kL = 7$ case. The

DR in $\gamma\gamma$ channel increases rapidly in the large $m_\phi = m_{h^0}$ region since $\Gamma_{h^0 \rightarrow \gamma\gamma}$ steeply decreases with increasing m_h due to the cancellation between top and W loops. So the $\gamma\gamma$ channel used in the search for the SH Higgs in the mass range 115-150 GeV by the LHC experiments is more sensitive for the ϕ search. Surprisingly large enhancements of DR in the $\gamma\gamma$ channel are predicted in this mass region in the $kL = 7$ case. This is because the $BF(\phi \rightarrow \gamma\gamma)$ is hugely enhanced in LRS model, as explained in the previous section. The ϕ should be detected in $\gamma\gamma$ in the current LHC data in the LRS scenario. This possibility is checked in Fig. 5.

The cross-section of a putative Higgs-boson signal, relative to the Standard Model cross section, as a function of the assumed Higgs boson mass, is widely used by the experimental groups to determine the allowed and excluded regions of m_{h^0} . By use of the DR in Fig. 4, we can determine the allowed region of m_ϕ from the present LHC data. Figure 5 shows the 95% confidence level upper limits on Higgs-like ϕ signals decaying into $\bar{X}X$ versus m_ϕ for $\bar{X}X = WW$ (ATLAS[41], CMS[42]) and $\gamma\gamma$ (ATLAS[43]).

For the LRS model with $kL = 7$, m_ϕ is excluded by ATLAS data at 95% CL over the m_ϕ range, $160 < m_\phi < 220$ GeV, while for RS model $kL = 35$ almost no regions of m_ϕ are yet excluded. Similar results are found from CMS data[42].

The ϕ search is also applicable to the Tevatron data. The CDF and D0 experiments excluded the SM Higgs with mass $158 \text{ GeV} < m_{h^0} < 175 \text{ GeV}$ from the data on WW, ZZ channels. The same data exclude ϕ in the $kL = 7$ case in m_ϕ range, $163 \text{ GeV} < m_\phi < 180 \text{ GeV}$, while for $kL = 35$, only $165 \text{ GeV} < m_\phi < 171 \text{ GeV}$ is excluded.

The $\gamma\gamma$ final state is very promising for ϕ detection, because the ϕ to h^0 detection ratio is generally very large in all the mass range of m_ϕ , as shown in Fig. 4. The $\gamma\gamma$ data of ATLAS do not show any resonance enhancements in $110 < m < 150 \text{ GeV}$ (*cf.* Fig. 5, so ϕ is excluded in this mass region in the LRS model ($kL = 7$) case, while no m_ϕ regions are excluded in the RS model with $kL = 35$.

For $m_\phi > 150 \text{ GeV}$, the $\gamma\gamma$ signal of h^0 is too small to be detected, but future data in this region can determine the existence of ϕ .

We take $\Lambda_\phi = 3 \text{ TeV}$ in our analyses. By taking larger values of Λ_ϕ , the detection ratios of ϕ decreases since the ϕ production cross section is proportional to $(1/\Lambda_\phi)^2$. By taking $\Lambda_\phi > 5 \text{ TeV}$, all values of m_ϕ become allowed by the latest ATLAS and CMS WW data, By taking $\Lambda_\phi > 10 \text{ TeV}$, all values of m_ϕ become allowed by the latest ATLAS $\gamma\gamma$ data,

A comment should be added here. There is a possible mixing effect[28] between

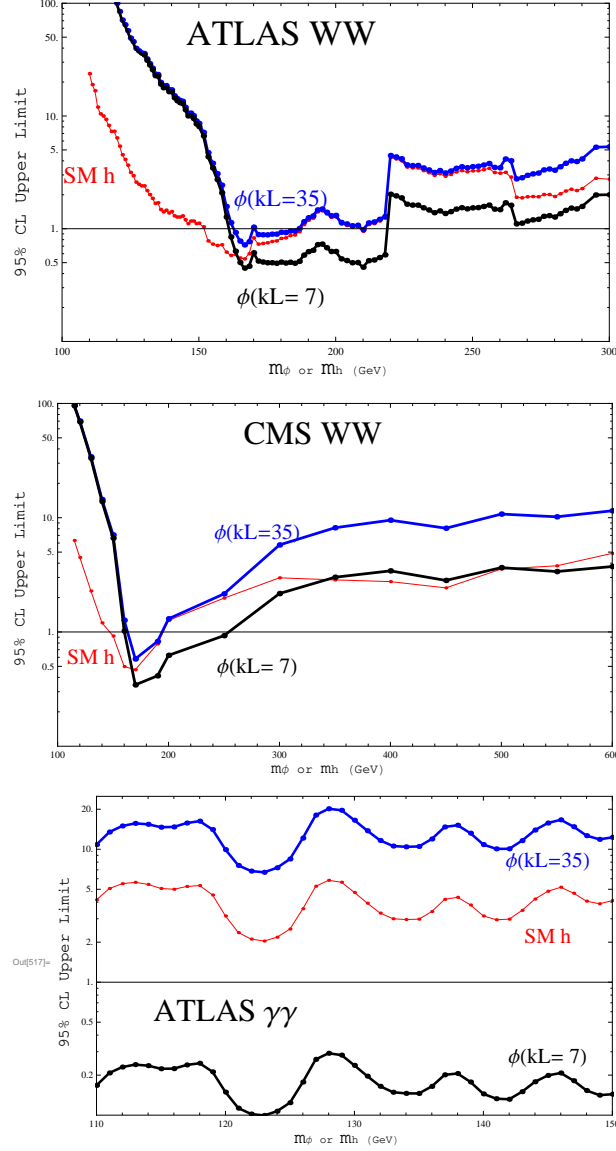


Fig. 5. the 95% confidence level upper limits on $(1/DR) \times (\sigma_{\text{exp}}/\sigma(h^0 \rightarrow \bar{X}X))$. This is the signal of a boson decaying into $\bar{X}X$ relative to the radion cross section $[\sigma(\phi \rightarrow \bar{X}X) = \sigma(h^0 \rightarrow \bar{X}X) \times DR]$ for $\bar{X}X = WW \rightarrow l\nu l\nu$ (ATLAS[41], CMS[42]) and $\gamma\gamma$ (ATLAS[43]) data. The cases $kL = 35$ (solid blue) and 7 (solid black) are shown. Similar results for the SM Higgs boson are also given (red thin-solid curve).

the radion and SM Higgs boson through the action

$$S_\xi = -\xi \int d^4x \sqrt{-g} R H^\dagger H \quad (13)$$

where H is Higgs doublet and $H = ((v + h^0)/\sqrt{2}, 0)$. Because of the Higgs-like nature of the radion coupling, its effect can be very large even if the mixing angle is very small. We have excluded wide m_ϕ -regions in LRS model with

$\Lambda_\phi = 3$ TeV in the no-mixing case. The effect of Eq. (13) is studied in detail in ref.[33] including a large ξ case of the RS1 model[31]. Generally speaking, when the $\text{BF}(\phi \rightarrow WW/ZZ)$ becomes larger(smaller) owing to the mixing effect, the $\text{BF}(\phi \rightarrow \gamma\gamma)$ becomes smaller(larger) than those in the no-mixing case. So the WW/ZZ and $\gamma\gamma$ channels are complementary for the detection of the radion.

6 Concluding Remarks

We have investigated the possibility of finding the radion ϕ at the Tevatron and LHC7. The radion can be discovered in the WW , ZZ , and $\gamma\gamma$ channels in the search for the SM Higgs h^0 . The WW detection rates can be comparable to that of the SM h^0 , in the mass region $m_\phi \sim 160$ GeV up to $2m_{h^0}$ as shown in Fig. 4. The $\gamma\gamma$ search channel is particularly promising, since the $\text{BF}(\phi \rightarrow \gamma\gamma)$ is almost constant at $\sim 10^{-4}$ for m_ϕ below 600 GeV, and the ϕ detection ratio compared to h^0 is very large above $m_\phi = 180$ GeV. Combining the $WW, \gamma\gamma$ data of ATLAS and CMS, the LRS model with $kL = 7$ is already excluded over wide ranges of m_ϕ for $\Lambda_\phi = 3$ TeV.

Acknowledgements

The authors would like to express their sincere thanks to Prof. W.-Y. Keung for his collaboration. M.I. is very grateful to the members of phenomenology institute of University of Wisconsin-Madison for hospitalities. This work was supported in part by the U.S. Department of Energy under grant No. DE-FG02-95ER40896, in part by KAKENHI(2274015, Grant-in-Aid for Young Scientists(B)) and in part by grant as Special Researcher of Meisei University.

References

- [1] L. Randall and R. Sundrum, Phys. Rev. Lett. **83**, 3370 (1999).
- [2] H. Davoudiasl, J. L. Hewett, and T. G. Rizzo, Phys. Lett. B **473**, 43 (2000).
- [3] A. Pomarol, Phys. Lett. B **486**, 153 (2000).
- [4] T. G. Rizzo, JHEP **0206**, 056 (2002).
- [5] C. Csaki, J. Hubisz, and S. J. Lee, Phys. Rev. D **76**, 125015 (2007).
- [6] Y. Grossman and M. Neubert, Phys. Lett. B **474**, 361 (2000).
- [7] K. Agashe, A. Delgado, M. J. May, and R. Sundrum, JHEP **08**, 050 (2003).

- [8] S. Chang, J. Hisano, H. Nakano, N. Okada, and M. Yamaguchi, Phys. Rev. D **62**, 084025 (2000).
- [9] C. Csaki, J. Erlich, and J. Terning, Phys. Rev. D **66**, 064021 (2002).
- [10] J. L. Hewett, F. J. Petriello, and T. G. Rizzo, JHEP **09**, 030 (2002).
- [11] C. Csaki, C. Grojean, L. Pilo and J. Terning, Phys. Rev. Lett. **92**, 101802 (2004).
- [12] R. Contino, Y. Nomura, and A. Pomarol, Nucl. Phys. B **671**, 148 (2003).
- [13] K. Agashe, R. Contino, and A. Pomarol, Nucl. Phys. B **719**, 165 (2005).
- [14] C. Csaki, C. Grojean, J. Hubisz, Y. Shirman, and J. Terning, Phys. Rev. D **70**, 015012 (2004).
- [15] T. Gherghetta and A. Pomarol, Nucl. Phys. B **586**, 141 (2000).
- [16] S. J. Huber and Q. Shafi, Phys. Lett. B **498**, 256 (2001).
- [17] G. Burdman, Phys. Rev. D **66**, 076003 (2002); Phys. Lett. B **590**, 86 (2004).
- [18] S. J. Huber, Nucl. Phys. B **666**, 269 (2003).
- [19] K. Agashe, G. Perez, and A. Soni, Phys. Rev. D **71**, 016002 (2005).
- [20] G. Cacciapaglia, C. Csaki, J. Galloway, G. Marandella, J. Terning, and J. Weiler, JHEP **04**, 006 (2008).
- [21] C. Csaki, A. Falkowski, and A. Weiler, JHEP **09**, 008 (2008).
- [22] S. Davidson, G. Isidori, and S. Uhlig, Phys. Lett. B **663**, 73 (2008).
- [23] W. D. Goldberger and M. B. Wise, Phys. Rev. Lett. **83**, 4922 (1999); Phys. Lett. B **475**, 275 (2000).
- [24] C. Csaki, M. L. Graesser, and G. D. Kribs, Phys. Rev. D **63**, 065002 (2001).
- [25] H. Davoudiasl, G. Perez, and A. Soni, Phys. Lett. B **665**, 67 (2008).
- [26] M. Bauer, S. Casagrande, L. Grunder, U. Haisch, and M. Neubert, Phys. Rev. D **76**, 076001 (2009).
- [27] H. Davoudiasl, T. McElmurry, and A. Soni, Phys. Rev. D **82**, 115028 (2010).
- [28] G. F. Giudice, R. Rattazzi, and J. D. Wells, Nucl. Phys. B **595**, 250 (2001).
- [29] Kingman Cheung, Phys. Rev. D **63**, 056007 (2001).
- [30] J. L. Hewett and T. G. Rizzo, JHEP **08**, 028 (2003).
- [31] D. Dominici, B. Grzadkowski, J. F. Gunion, and M. Toharia, Nucl. Phys. B **671**, 243 (2003); Acta Phys. Pol. B **33**, 2507 (2002).
- [32] J. F. Gunion, M. Toharia, and J. D. Wells, Phys. Lett. B **585**, 295 (2004).

- [33] M. Toharia, Phys. Rev. **D79**, 015009 (2009).
- [34] S. Casagrande, F. Goertz, U. Haisch, M. Neubert, and T. Pfoh, JHEP **10**, 094 (2008).
- [35] M. Frank, B. Korutlu, and M. Toharia, arXiv:1110.4434v1 [hep-ph].
- [36] J. Baglio and A. Djouadi, arXiv:1012.0530v3 [hep-ph].
- [37] S. Catani, D. de Florian, M. Grazzini, and P. Nason, JHEP**07**, 028 (2003)
- [38] W.-Y. Keung and W. J. Marciano, Phys. Rev. **D30**, 248 (1984).
- [39] "The Higgs Hunters' Guide," J. F. Gunion, H. E. Haber, G. Kane, and S. Dawson, Perseus books 1990.
- [40] V. D. Barger and R. J. N. Phillips, "Collider Physics" Updated Edition, Westview press (1991).
- [41] The ATLAS Collaboration, preliminary result given in the presentation by M. L.Vazquez Acosta in SUSY2011 at FNAL, Aug. 30, 2011
- [42] The CMS Collaboration, "Search for the Higgs Boson Decaying to W+W in the Fully Leptonic Final State". CMS physics result, 18-Aug-2011, for the analysis CMS-HIG-11-014 on CMS public web.
- [43] The ATLAS Collaboration, CERN-PH-EP-2011-129; arXiv:1108.5895v1 .
- [44] M. Schreck and M. Steinhauser, arXiv:0708.0916v2 [hep-ph].